arXiv:astro-ph/0005123 v3 2 Oct 2000

MAXIMA-1: A MEASUREMENT OF THE COSMIC MICROWAVE BACKGROUND ANISOTROPY ON ANGULAR SCALES OF 10′ TO 5°

S. Hanany[1,2], P. Ade[3], A. Balbi[4,2,15], J. Bock[5,6], J. Borrill[2,7], A. Boscaleri[8], P. de Bernardis[9], P. G. Ferreira[10,11], V. V. Hristov[6], A. H. Jaffe[2], A. E. Lange[2,6], A. T. Lee[14,15,2], P. D. Mauskopf[12], C. B. Netterfield[13], S. Oh[2], E. Pascale[8], B. Rabii[2,14], P. L. Richards[2,14], G. F. Smoot[2,14,15,16], R. Stompor[2,16,17], C. D. Winant[2,14], J. H. P. Wu[18]

Draft version June 4, 2005

ABSTRACT

We present a map and an angular power spectrum of the anisotropy of the cosmic microwave background (CMB) from the first flight of MAXIMA. MAXIMA is a balloon-borne experiment with an array of 16 bolometric photometers operated at 100 mK. MAXIMA observed a 124 deg^2 region of the sky with 10′ resolution at frequencies of 150, 240 and 410 GHz. The data were calibrated using in-flight measurements of the CMB dipole anisotropy. A map of the CMB anisotropy was produced from three 150 and one 240 GHz photometer without need for foreground subtractions. Analysis of this CMB map yields a power spectrum for the CMB anisotropy over the range $36 \leq \ell \leq 785$. The spectrum shows a peak with an amplitude of 78 ± 6 μK at $\ell \simeq 220$ and an amplitude varying between ~ 40 μK and ~ 50 μK for $400 \lesssim \ell \lesssim 785$.

Subject headings: cosmic microwave background - cosmology: observations

1. INTRODUCTION

Measurements of the anisotropy of the cosmic microwave background (CMB) can discriminate between cosmological models and determine cosmological parameters with high accuracy (Kamionkowski & Kosowsky 1999, and references therein). Inflationary dark matter models, for example, predict a series of peaks in the angular power spectrum of the anisotropy. The collected results from many experiments show the existence of a first peak at angular scales corresponding to the spherical harmonic multipole number $\ell \sim 200$. These results have been interpreted as evidence for a flat universe (de Bernardis et al. 2000; Lange et al. 2000; Dodelson & Knox 2000; Tegmark & Zaldarriaga 2000; Pierpaoli, Scott, & White 2000). Additional observations probing a broad range of angular scales would greatly increase confidence in these results and further constrain cosmological parameters.

MAXIMA is a balloon-borne experiment optimized to map the CMB anisotropy over hundreds of square degrees with an angular resolution of 10′. In this paper we report results from the MAXIMA-1 flight which took place on August 2, 1998. These include a 100 square degrees map of the CMB anisotropy and the resulting power spectrum over the range $36 \leq \ell \leq 785$, which is the largest range reported to date. Despite several common team members, the data analysis was independent of that leading to the recently reported BOOMERANG results (de Bernardis et al. 2000). A companion paper, Balbi et al. (2000), discusses the cosmological significance of the MAXIMA-1 results.

2. INSTRUMENTATION

Lee et al. (1999) gives a detailed description of the MAXIMA system. It is based on a well-baffled, under-filled, off-axis Gregorian telescope with a 1.3 m primary mirror, mounted on an attitude-controlled balloon-borne platform. A well-baffled liquid-Helium-cooled optics box is lined with absorbing material (Bock 1994) and con-

[1]School of Physics and Astronomy, University of Minnesota/Twin Cities, Minneapolis, MN, USA

[2]Center for Particle Astrophysics, University of California, Berkeley, CA, USA

[3]Queen Mary and Westfield College, London, UK

[4]Dipartimento di Fisica, Università Tor Vergata, Roma, Italy

[5]Jet Propulsion Laboratory, Pasadena, CA, USA

[6]California Institute of Technology, Pasadena, CA, USA

[7]National Energy Research Scientific Computing Center, Lawrence Berkeley National Laboratory, Berkeley, CA, USA

[8]IROE-CNR, Firenze, Italy

[9]Dipartimento di Fisica, Università La Sapienza, Roma, Italy

[10]Astrophysics, University of Oxford, Oxford, UK

[11]CENTRA, Instituto Superior Tecnico, Lisboa, Portugal

[12]Department of Physics and Astronomy, University of Wales, Cardiff, UK

[13]Dept. of Physics and Astronomy, University of Toronto, Canada

[14]Dept. of Physics, University of California, Berkeley CA, USA

[15]Division of Physics,Lawrence Berkeley National Laboratory, Berkeley, CA, USA

[16]Space Sciences Laboratory, University of Californina, Berkeley, CA, USA

[17]Copernicus Atronomical Center, Warszawa, Poland

[18]Department of Astronomy, University of California, Berkeley, CA, USA

1

ν_0	$[\nu_{min},\nu_{max}]$	FWHM[a]	τ	NET
(GHz)	(GHz)	(arcmin)	(msec)	($\mu K\sqrt{sec}$)
150	[120, 190]	(11.5,10)	10	80
150	[120, 190]	(10.5,9.5)	7	90
150	[120, 190]	(11.5,9.5)	7	90
240	[190, 270]	(12,8.5)	7	120
410	[380, 430]	(11,8)	6	2050

[a] The beams have some asymmetry. The FWHM are for the long and short axes.

TABLE 1

CENTRAL FREQUENCIES (ν_0), FREQUENCY BANDS (ν_{min},ν_{max}), BEAM FULL WIDTHS AT HALF MAXIMUM (FWHM), DETECTOR TIME CONSTANTS (τ), AND DETECTOR NOISE EQUIVALENT TEMPERATURES (NET) IN CMB THERMODYNAMIC UNITS FOR THE FIVE MAXIMA-1 PHOTOMETERS DISCUSSED IN THIS PAPER. THE FWHM, τ, AND NET WERE DETERMINED USING FLIGHT DATA. THE FREQUENCY BANDS WERE MEASURED IN THE LABORATORY.

tains two reimaging mirrors, low-pass filters, field and aperture stops, feed horns for the 16 photometers, and a focal-plane stimulator. Eight conical single-mode horns at 150 GHz and four multi-mode Winston horns each at 240 GHz and 410 GHz provide 10′ beams at all three frequencies. The frequency bands are defined with absorptive and metal-mesh filters. Radiation is detected with spider-web bolometers (Bock et al. 1996) operated at 0.1 K with an adiabatic demagnetization refrigerator (Hagmann & Richards 1995). The bolometers are AC-biased to avoid low-frequency amplifier noise. Additional channels with a constant resistor, a thermometer, and a dark bolometer are used to monitor electromagnetic interference, cross-talk, and drifts in electronic gain and temperature. The gondola azimuth is driven by a reaction wheel using information from a two-axis magnetometer and a three-axis rate gyroscope. The telescope elevation is set using information from an angle encoder. Observations were carried out at fixed elevation with the primary mirror scanning $\pm \sim 2°$ in azimuth at 0.45 Hz and the gondola also scanning in azimuth but at a frequency of ~ 0.02 Hz. Both scans were triangle functions of time with smoothed turnarounds.

3. OBSERVATIONS

The MAXIMA-1 flight was launched from the National Scientific Balloon Facility in Palestine, Texas at 1 UT on August 2, 1998. Observations of the CMB dipole for the purpose of calibration began at 3.6 UT when the payload reached an altitude of 32 km and ended at 4.2 UT after ~ 100 rotations at 3.3 rpm. The elevation angle was set to 51°. The payload reached float altitude of 38.4 ± 0.4 km at 4.6 UT.

The 1.6 hour CMB-1 observation began at 4.35 UT with a telescope elevation of 46.3°. The gondola was scanned $\pm 4.1°$ in azimuth at 16.1 mHz centered at 321.5°. The 1.4 hour CMB-2 observation began at 6.0 UT with a telescope elevation of 32.3°. The gondola was scanned $\pm 2.9°$ at 21.3 mHz centered at 323°. Because of sky rotation, the combination of these observations covered a nearly square region of the sky with an area of 124 square degrees of which 45% is cross-linked at an angle of $\sim 22°$.

Observations of Jupiter were carried out from 7.5 to 8.1 UT to map the telescope beams and provide additional calibration information. The elevation was fixed at 44.2° while sky rotation and the primary mirror modulation provided ~ 200 transits across each beam.

4. POINTING RECONSTRUCTION AND CALIBRATION

We identified the stars which moved through the field of a CCD camera aligned with the center of the primary mirror scan by using the balloon location, telescope elevation, and the position of Polaris in an offset CCD camera. Interpolations using an angle encoder on the primary mirror, rate gyroscopes, and the known star positions permitted pointing reconstruction to better than 1′ RMS. Less than 0.1% of the data had pointing uncertainty larger than 2′ and were not used.

A full beam calibration of the 150 and 240 GHz photometers was obtained from observations of the CMB dipole. The data from each rotation were χ^2-fitted to a linear combination of a dipole model (Lineweaver et al. 1996), a galactic-dust emission model (Schlegel, Finkbeiner, & Davis 1998), data from one 410 GHz photometer, an offset, and a gradient. The amplitude of each of these components was treated as a free parameter. A monotonic change in the detector calibration of less than 9% throughout the CMB observations, due to an increasing detector temperature, was monitored by illuminating the focal plane with the stimulator lamp. Estimated 1σ calibration uncertainties were less than 4% for each of the 150 and 240 GHz photometers. The uncertainties in the dipole calibration and the time dependent calibration contributed about equally to the total error, and systematic sources contributed about 25%.

Beam maps and an independent calibration were obtained from observations of Jupiter. We estimate a 1σ uncertainty of $\pm 0.5'$ in the size of the beams. The beam profiles were integrated and used with the angular diameter and brightness temperature of Jupiter (Goldin et al. 1997) and the optical bandpass functions to calibrate all 16 photometers. For the data reported here, the errors in the calibration from Jupiter were between 12 and 14% (with about 10, 5, 5, and 2% coming from uncertainties in the beam solid angle, frequency bands, Jupiter's flux, and measured signal, respectively). The absolute calibrations from the dipole agreed with those from Jupiter to within 1σ, with the Jupiter calibration predicting larger temperature fluctuations by 11 to 14%.

5. MAP AND ANGULAR POWER SPECTRUM

In this paper we report on the analysis of data from the three 150 GHz, one 240 GHz, and one 410 GHz photometer described in Table 1. At 150 and 240 GHz these photometers are the most sensitive in the MAXIMA array and give the highest sensitivity of any CMB instrument reported to date.

The raw data for each photometer consisted of 2.3 million samples of which about 16% were not used. We removed the stimulator calibration events and other events with an amplitude larger than 6σ. This procedure broke the data into 20 segments that were treated as independent observations of the sky. Samples in each of the segments which were in excess of 4σ, such as cosmic ray hits and short telemetry drop-outs, were removed. For the data of one of the photometers, we repeated the data analysis by using a threshold of 3σ with no significant change in the resulting angular power spectrum. We deconvolved the transfer functions of the bolometers and readout electronics and estimated the noise power spectrum from sections of the time stream that had no gaps (Stompor et al., in preparation). We used the procedure of Ferreira & Jaffe (2000) to confirm that the time-domain data are dominated by noise. We marginalized over frequencies lower than 0.1 Hz and higher than 30 Hz, where we did not expect appreciable optical signals.

The calibrated time stream data were combined with the pointing solution to produce a maximum likelihood pixelized map of temperature anisotropy and a pixel-pixel noise correlation matrix for each photometer (Wright 1996; Tegmark 1997; Bond et al. 1999). An area of ~ 20 square degrees of the map was not well cross-linked and is not included in the present analysis. The data showed a signal that was phase-synchronous with the primary mirror scan which was due to radio-frequency interference from on-board transmitters modulated by the mirror motion. This signal was constant within each data segment, varied between different photometers, and had an amplitude of 100 - 300 μK. We removed it by allocating fictitious map pixels to values of the primary mirror angle and determined the maximum likelihood map in these pixels simultaneously with the temperature anisotropy map (Stompor et al., in preparation).

We verified that there are no noise correlations between maps of different photometers by producing difference maps from the data of pairs of photometers. The angular power spectra of these maps were consistent with no signal. We also showed that histograms of the temperatures in the difference maps were consistent with the distributions expected for no noise correlations at a Kolmogorov-Smirnov significance level larger than 10%. A combined temperature anisotropy map was then produced by adding individual maps with a weight inversely proportional to their noise correlation matrices. A Wiener filtered version of this map is shown in Figure 1. We assign a calibration uncertainty of 4% to the magnitude of temperature fluctuations in the combined map.

We calculated the angular power spectrum C_ℓ of the combined map using the MADCAP (Borrill 1999) implementation of the maximization of the likelihood function following Bond, Jaffe & Knox (1998). This implementation assumes that the beam shape has axial symmetry.

We produced an effective beam for the analysis of the combined map by noise-weight averaging the individual beams. We followed the procedure of Wu et al. (2000) to find a symmetric approximation for the effective beam and included the small smoothing provided by the pixelization. We tested this procedure for the MAXIMA-1 beams and data and found no systematic bias of the C_ℓ estimates (Wu et al. 2000) . We calculated the power spectrum of the temperature fluctuations using 15 bins in ℓ over the range $3 \lesssim \ell \lesssim 1500$ assuming a constant $\ell(\ell+1)C_\ell$ band power in each bin, and marginalizing over the CMB monopole and dipole. We further marginalized over the bins at $\ell < 35$ and $\ell > 785$ and diagonalized the ℓ-bin correlation matrix using a variant of techniques discussed in Bond, Jaffe & Knox (1998). The correlations between the dominant bin and adjacent bins were typically less than 10%. Table 2 lists the dominant bins, the C_ℓ estimates, and the $\Delta T = \sqrt{\ell(\ell+1)C_\ell/2\pi}$ estimates for the corresponding uncorrelated linear combinations of bins. We quote 1σ errors on the C_ℓ estimates assuming 68% confidence intervals using the offset log-normal distribution model of Bond, Jaffe & Knox (2000). These errors do not include two additional independent sources of uncertainty. Expressed as a percentage of $\ell(\ell+1)C_\ell/2\pi$, the 1σ calibration error is a constant 8% and the ℓ-dependent error due to the beam-diameter uncertainty, which has been shown to be fully correlated between ℓ bins, is given in Table 2. Information on the shape of the bin-power likelihood functions and window functions will be made available on the MAXIMA web site (http://cfpa.berkeley.edu/maxima).

The top panel of Figure 2 shows the maximum likelihood power spectrum, an inflationary adiabatic model that best fits the MAXIMA-1 and COBE/DMR power spectra, and a ΛCDM model. The χ^2 for the best fit and for the ΛCDM models are 41 and 50, respectively, using all 38 data points. If we only use the 10 data points of MAXIMA-1 we obtain $\chi^2 = 7$ and 9 for the best fit and ΛCDM, respectively (Balbi et al. 2000).

6. FOREGROUNDS

Foreground sources include emission from the earth, the atmosphere, interstellar dust, free-free radiation, synchrotron radiation, and point sources, and scattering due to the Sunyaev-Zeldovich effect. The two CMB scans, performed with a separation of 1.5 hours at different telescope elevations, show consistent structure. This temporal stability is inconsistent with an atmospheric or ground-based origin for the signal. We extrapolated the 100 μm, $10'$ resolution Schlegel, Finkbeiner, & Davis (1998) map of our observed region to lower frequencies using the two-component dust model favored by Finkbeiner, Davis & Schlegel (1999). The predicted RMS dust temperature is only 2.3 and 9.3 μK, for the 150 and 240 GHz bands, respectively. We found a statistically significant correlation between the dust model and our maps. The ratio of the detected to predicted RMS dust signal was statistically consistent with unity. When we subtracted the correlated dust signal from the maps the change in the measured angular power spectrum was negligible. A catalog search (Sokasian, Gawiser, & Smoot 2000; Gawiser & Smoot 1997) yielded no detectable radio or infrared sources in any of the frequency bands. Estimates

ℓ_{eff}	$[\ell_{min}, \ell_{max}]$	$\ell(\ell+1)C_\ell/2\pi$ (μK^2)	Beam Error (%)	ΔT (μK)
77	[36, 110]	2000^{+680}_{-510}	± 0	45^{+7}_{-6}
147	[111, 185]	2960^{+680}_{-550}	± 0.5	54^{+6}_{-5}
223	[186, 260]	6070^{+1040}_{-900}	± 1.5	78^{+6}_{-6}
300	[261, 335]	3720^{+620}_{-540}	± 2.5	61^{+5}_{-5}
374	[336, 410]	2270^{+390}_{-340}	± 3.5	48^{+4}_{-4}
447	[411, 485]	1530^{+310}_{-270}	$^{+5}_{-4.5}$	39^{+4}_{-4}
522	[486, 560]	2340^{+430}_{-380}	$^{+6.5}_{-6}$	48^{+4}_{-4}
597	[561, 635]	1530^{+380}_{-340}	$^{+8}_{-7}$	39^{+5}_{-5}
671	[636, 710]	1830^{+490}_{-440}	$^{+9.5}_{-8.5}$	43^{+5}_{-5}
742	[711, 785]	2180^{+700}_{-620}	$^{+11}_{-10}$	47^{+7}_{-7}

TABLE 2

UNCORRELATED POWER SPECTRUM FROM THE MAXIMA-1 MAP. ERRORS ARE THE 68% INTEGRATED PROBABILITY OF THE OFFSET LOG-NORMAL LIKELIHOOD FUNCTIONS WITH A CONSTANT PRIOR IN EITHER $\ell(\ell+1)C_\ell/2\pi$ OR $\Delta T = \sqrt{\ell(\ell+1)C_\ell/2\pi}$ FOR THEIR RESPECTIVE COLUMNS. HERE $[\ell_{min}, \ell_{max}]$ GIVES THE RANGES OF THE DOMINANT BINS. THE CORRELATED BEAM ERRORS ARE DESCRIBED IN THE TEXT.

of bremsstrahlung and synchrotron radiation (Bouchet & Gispert 1999) yielded contributions of less than 1 μK at 150 and 240 GHz and no subtractions were made.

Integrating the measured power spectrum of one photometer at 150 GHz and the one at 240 GHz we find for a thermodynamic temperature fluctuations ratio of 0.91 ± 0.18 compared to unity for the CMB, 0.06 for emission from dust, 2.1 for synchrotron, and 3.7 for free-free radiation, assuming the Tegmark et al. (2000) "middle" foregrounds model. For the ratio between 150 and 410 GHz, we found a lower limit of $1.1 \cdot 10^{-2}$ compared to $3.2 \cdot 10^{-4}$ for dust and $5.7 \cdot 10^{-5}$ for atmosphere. The observed anisotropy is not consistent with the thermal SZ effect, which would produce anti-correlated structure in the 150 and 240 GHz bands.

7. TESTS FOR SYSTEMATIC ERRORS

Because of computational limitations, tests for systematic errors were done with maps which had square pixels of $8'$ and $10'$ on a side. The power spectra calculated from the $8'$-pixel and $5'$-pixel combined maps were statistically consistent. The following combinations of the data were analyzed and produced a power spectrum consistent with no signal: (1) a dark bolometer, (2) the data from the 410 GHz photometer, (3) the difference between the overlapping part of the combined map from the CMB-1 and -2 scans, (4) the differences between the maps produced by different photometers. We also weight-averaged the maps of the second and third photometers in Table 1 and the first and fourth. The maximum likelihood estimate of the power spectrum of the difference between these independent maps is consistent with no signal as shown by the open circles in the top panel of Figure 2.

We compared the estimate of the angular power spectrum to that obtained using: (1) only the sections of the map where the CMB-1 and -2 scans overlap, (2) a map of each of the CMB scans alone. We made maps and calculated C_ℓ estimates from the data of each photometer alone and using: (1) only a sub-section of the time stream data, (2) a high-pass filtered version of the time stream where

the high-pass was a time domain box-car with a width of 10 sec, (3) various combinations of frequency marginalizations between 30 and 70 Hz, and 0.05 and 0.3 Hz, respectively. In all these cases the computed power spectra agreed among themselves and with the power spectrum presented in this paper. The Kolmogorov-Smirnov test (see Section 5), as applied to difference maps and to a map of the dark bolometer, confirms that we correctly estimated the noise in the experiment and that the pixel-domain noise is Gaussian.

We used simulations to test the algorithm used to subtract the signal that was phase-synchronous with the primary mirror modulation. We found that the power spectrum estimate was not biased with phase-synchronous signals larger than those observed in the data. If we make the maps without removing the phase-synchronous signal the power spectrum estimate changes only at $\ell \lesssim 200$.

The computer programs used to generate the maps and power spectra were tested extensively using simulations of the time domain data and noise. Maps were produced by two independent computer codes and the power spectra calculated from these maps were consistent. We used one of the map-making codes to make maps of Jupiter and found them consistent with those obtained with a simple data-binning technique.

8. DISCUSSION

We have observed temperature anisotropy on the sky at 150 and 240 GHz that is consistent with fluctuations in the cosmic microwave background radiation, and inconsistent with any known foreground. The observations were carried out with photometers that give the highest CMB sensitivity reported to date. Our measurements cover a range of angular scales corresponding to the multipole range $36 \leq \ell \leq 785$, which is the largest yet reported by a single experiment. The measured angular power spectrum shows a clear peak at $\ell \simeq 220$, and an amplitude varying between ~ 40 μK and ~ 50 μK at $400 \lesssim \ell \lesssim 785$. The power spectrum is well fit by an inflationary adiabatic model over the entire range of ℓ. The best-fit model

has a total energy density close to unity and a non-zero cosmological constant. The MAXIMA-1 power spectrum appears consistent with that of the BOOMERANG experiment (de Bernardis et al. 2000) once the power spectra of the two experiments are scaled by factors equal to their respective 1σ calibration uncertainties, see Figure 2. A detailed analysis of the combined data sets which includes a determination of the calibration factors that bring the experiments to agreement is presented in Jaffe et al. (2000).

REFERENCES

Balbi, A., *et al.* 2000, ApJ, submitted
Bock, J. J. 1994, Ph.D. Thesis, UC Berkeley, Berkeley, CA
Bock J. J., DelCastillo, H. M., Turner, A. D., Beeman, J. W., Lange, A. E., & Mauskopf, P. D. 1996, Proc. of 30th ESLAB Symp., 'Submillimeter and Far-Infrared Space Instrumentation', ESTEC, Noordwijk, ESA, SP-388.
Bond, J. R., Crittenden, R., Jaffe, A. H., & Knox, L. E. 1999, Computing in Science and Engineering, 1, 21, astro-ph/9903166.
Bond, J. R., Jaffe, A. H., & Knox, L. 1998, Phys. Rev. D, 57, 2117, astro-ph/9708203
Bond, J. R., Jaffe, A. H., & Knox, L. 2000, ApJ, 533, 19 astro-ph/9808264
Borrill, J. 1999, in EC-TMR Conference Procedings 476, 3K Cosmology, ed. L. Maiani, F. Melchiorri, & N. Vittorio (Woodbury, New York: AIP), 224
Bouchet, F., & Gispert, R. 1999, New Astronomy, 4, 443
de Bernardis, P., et al. 2000, Nature, 404, 995
Dodelson, S., & Knox, L. 2000, Phys. Rev. Let, 84 3523
Ferreira, P. G., & Jaffe, A. H. 2000, MNRAS, 312, 89, astro-ph/9909250
Finkbeiner, D. P., Davis, M., & Schlegel, D. J. 1999, ApJ, 524, 867
Gawiser, E., & Smoot G. 1998, ApJ, 480L, 1, astro-ph/9603121
Goldin, A. B., *et al.* 1997, ApJ, 488L, 161, astro-ph/9612040

Hagmann, C., & Richards, P. L. 1995, Cryogenics, 35, 303
Hanany, S., Jaffe, A. H., & Scannapieco, E. 1998, MNRAS, 299, 653
Jaffe, A. H., *et al.* 2000, Phys. Rev. Let, submitted, astro-ph/0007333
Kamionkowski, M., & Kosowsky, A. 1999, Annual Reviews of Nuclear and Particle Science, in press, astro-ph/9904108
Lange, A. E., *et al.* 2000, Phys. Rev D., submitted
Lee, A. T., *et al.* 1999, in EC-TMR Conference Procedings 476, 3K Cosmology, ed. L. Maiani, F. Melchiorri, & N. Vittorio (Woodbury, New York: AIP), 224, astro-ph/9903249
Lineweaver, C. H., Tenorio, L., Smoot, G. F., Keegstra, P., Banday, A. J., & Lubin, P. 1996, ApJ, 470, 38L
Pierpaoli, E., Scott, D., & White, M. 2000, Science, 287, 2171
Schlegel D. J., Finkbeiner, D. P. & Davis, M. 1998, ApJ, 500, 525
Sokasian, A., Gawiser, E. & Smoot G. 2000, ApJ, submitted. astro-ph/9811311
Tegmark, M. 1997, ApJ, 480, 87
Tegmark, M., Eisenstein, D., Hu, W., & De Oliveira-Costa, A. 2000, ApJ, 530, 133, astro-ph/9905257
Tegmark, M., & Zaldarriaga, M., 2000, ApJ, submitted, astro-ph/0002091
Wright, E. L. 1996, astro-ph/9612006
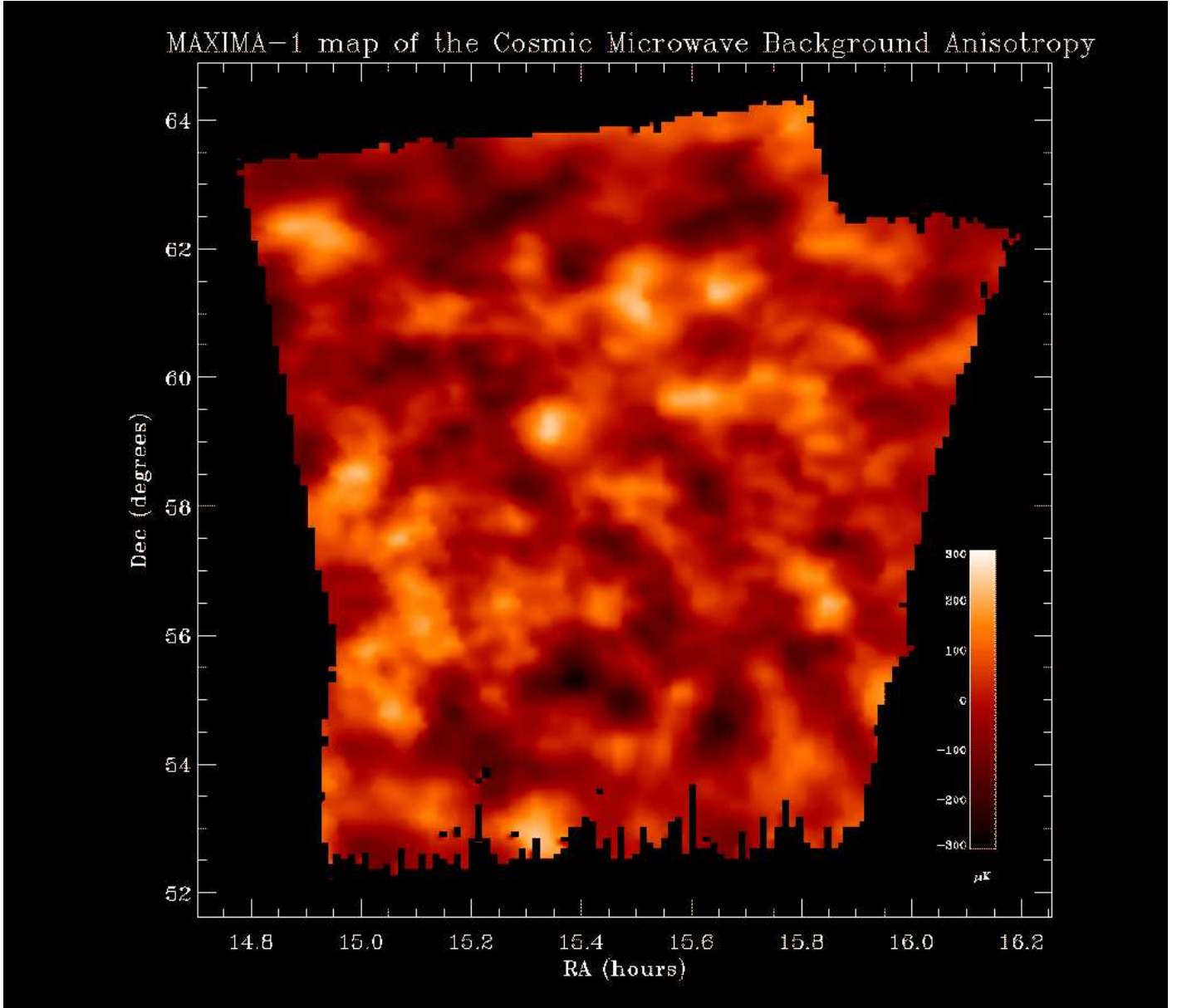Wu, J. H. P., *et al.* 2000, ApJ, submitted, astro-ph/0007212

6

FIG. 1.— A Wiener filtered map of the CMB anisotropy with 10′ resolution from MAXIMA-1. The map is made using data from three 150 GHz and one 240 GHz photometer and contains 15,000 5′×5′ pixels. We used the angular power spectrum shown in the top panel of Figure 2 as the prior for the Wiener filter. Pixel boundaries have been smoothed using interpolation.
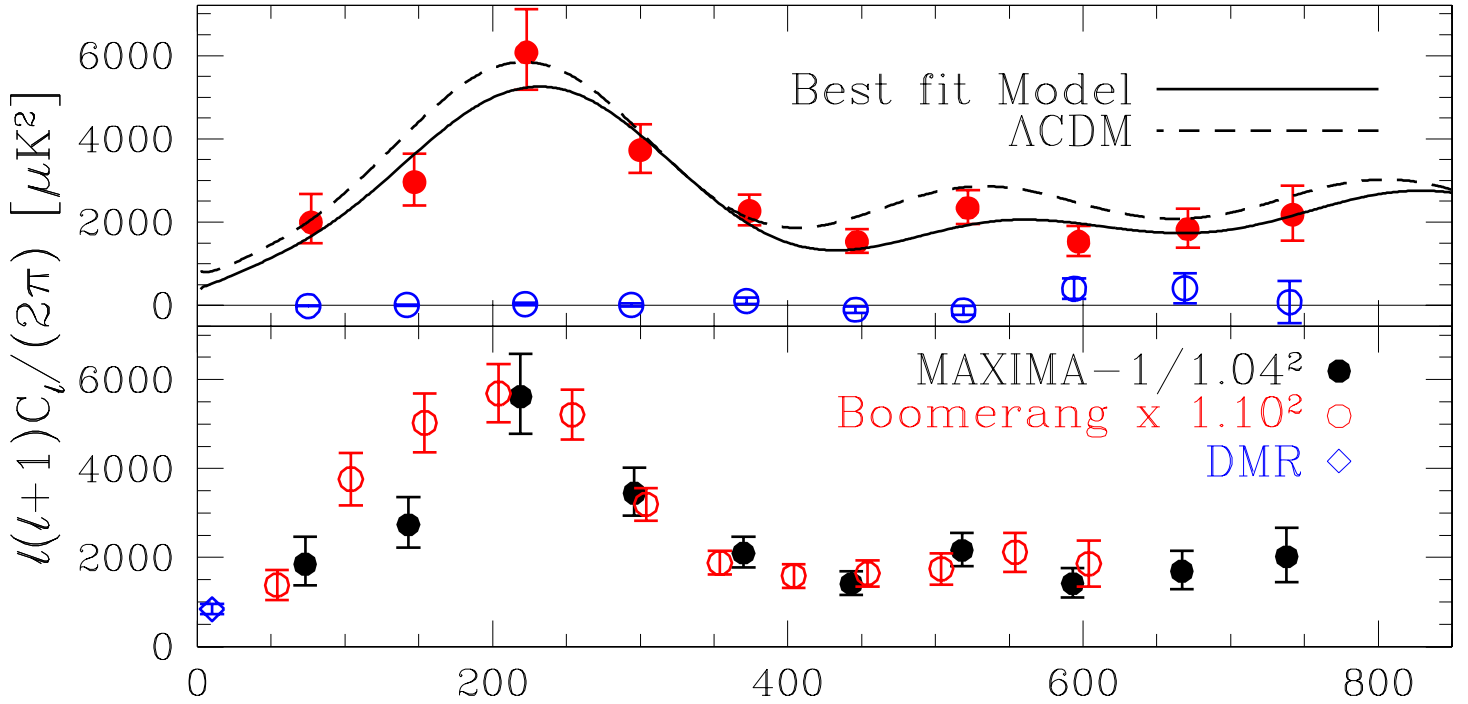
FIG. 2.— Top panel: Angular power spectrum of the CMB anisotropy from the MAXIMA-1 map shown, in Figure 1 (filled circles). The error bars are 68% confidence intervals calculated using the offset log-normal likelihood functions of Bond, Jaffe & Knox (2000). The solid (dashed) curve is the best fit (ΛCDM) inflationary adiabatic cosmology to the MAXIMA-1 and COBE/DMR data. The models have $(\Omega_b, \Omega_{cdm}, \Omega_\Lambda, n, h) = (0.1, 0.6, 0.3, 1.08, 0.53)$, and $(0.05, 0.35, 0.6, 1, 0.65)$, respectively (Balbi et al. 2000). The open circles are the estimated power spectrum of the difference between two independent maps, each produced by a weighted-average of the maps from a pair of photometers. Bottom panel: A comparison of the MAXIMA power spectrum with that of the recently reported BOOMERANG experiment (de Bernardis et al. 2000). Consistency between the power spectra has been achieved by scaling the MAXIMA-1 (BOOMERANG) power spectrum down (up) by a factor equal to its 8% (20%) 1σ calibration uncertainty. These data show a suggestion of a peak at $\ell \sim 525$.